



ELSEVIER

15 May 2001

OPTICS
COMMUNICATIONS

Optics Communications 192 (2001) 77–81

www.elsevier.com/locate/optcom

Optoelectronic delayed-feedback and chaos in quantum-well laser diodes

C. Juang^{a,*}, C.C. Huang^b, T.M. Hwang^c, J. Juang^d, W.W. Lin^b

^a Department of Electronics, Ming Hsin College, Hsinfeng, Hsinchu, Taiwan, ROC

^b Department of Mathematics, National Tsing Hua University, Hsinchu, Taiwan, ROC

^c Department of Applied Mathematics, I-Shou University, Kaohsiung, Taiwan, ROC

^d Department of Applied Mathematics, National Chiao Tung University, Hsinchu, Taiwan, ROC

Received 14 September 2000; received in revised form 8 November 2000; accepted 14 March 2001

Abstract

Electronic-controlled route to chaos in a quantum-well laser diode is carried out by a delayed-feedback technique. By introducing an extra delayed-feedback control term $cS_n(t - \tau)$, chaotic light output can be achieved at relatively low bias and small modulation depth. Bifurcation diagram, Poincaré map, and Lyapunov exponents suggests quasi-periodicity route to chaos. © 2001 Elsevier Science B.V. All rights reserved.

PACS: 42.55.Px; 42.65.Sf; 05.45.Pq

Keywords: Chaos; Lyapunov exponents; Quantum-well laser diodes; Delay differential equation

Dynamical chaos in laser diodes has become an interesting topic due to its potential application in private communication [1,2]. Chaotic light output from a laser diode can be achieved by optical- or electronic-controlled techniques. Optical-controlled technique includes optical feedback using an external cavity [3] or by an optical injection from a second laser diode [4]. Electronic-controlled technique is carried out by injecting a sinusoidal and a bias current into the laser diode $I = a + b \sin 2\pi f_0 t$, where a is the bias current, b is the modulation current, f_0 is the external modulation frequency [5,6]. In general, high bias and

strong current modulation, or two tone modulation are required to achieve chaos.

Electronic-controlled route to chaos in a laser diode can be further expanded using a delayed-feedback technique. This delay technique has also been used to optical-controlled route to chaos in a laser diode [7]. Hopf bifurcation subject to a large delay is also verified [8]. In this work, the electronic delayed-feedback technique is applied to a quantum-well laser diode. A PIN photodetector can be placed at the other side of the facet of the laser diode, as the case of most commercial laser diodes. The photocurrent is proportional to the output photon density $S_n(t)$. Since the chaotic output is always a broadband signal, the bandwidth of the photodetector should be high enough to ensure the coverage of the chaotic spectra. An electronic

* Corresponding author. Fax: +886-3-559-1402.

E-mail address: cjuang@mh.it.edu.tw (C. Juang).

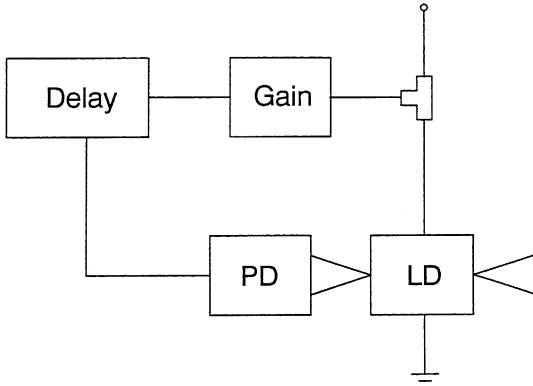


Fig. 1. Schematic diagram of a laser diode using delay-time feedback control.

delayed-feedback loop is then established by leading the photocurrent to a delayed-time circuit and a gain stage, and then mixing with the sinusoidal input, as illustrated in Fig. 1. The overall current is then injected into the laser diode and is given by

$$I = a + b \sin 2\pi f_0 t + c S_n(t - \tau), \quad (1)$$

where c is the current gain, and τ is the loop delay time. With the introduction of the extra delay term $c S_n(t - \tau)$, it is shown that the chaotic light output can be obtained at relatively low bias and small modulation depth. Note that without modulation and delay, the system always converges to a fixed point. With delay only or small modulation depth only, it is not possible to achieve chaos. The interaction between modulation and delay forms a quasi-two-period route to chaos. These chaotic behaviors are further investigated by bifurcation diagram, Poincaré map, and Lyapunov exponent.

The three-dimensional quantum-well rate equation to describe the dynamics of carrier in separate confinement regions I_s , in quantum well region I_n , and photon density S_n using the delayed-feedback technique is given by [9]

$$\begin{aligned} \tau_s \frac{dI_s}{dt} &= a + b \sin 2\pi f_0 t + c S_n(t - \tau) - \left(1 + \frac{\tau_s}{\tau_n}\right) I_s, \\ \tau_n \frac{dI_n}{dt} &= I_s - I_n - G(1 - \epsilon_n S_n) S_n, \\ \frac{C_p}{\Gamma} \frac{dS_n}{dt} &= G(1 - \epsilon_n S_n) S_n + \beta I_n - \frac{S_n}{\Gamma R_p}, \end{aligned} \quad (2)$$

Table 1

The parameters used for the simulation of quantum-well lasers

Parameters	Value	Unit
τ_s	6	ps
τ_n	2.25	ns
ϵ	10^{-17}	cm^3
Γ	0.2	–
R_p	59.5	Ω
C_p	0.0489	pf
β	10^{-4}	–
D	1.79×10^{-29}	$\text{V}^{-1} \text{A}^{-1} \text{m}^6$
qV_a	6.85×10^{-35}	$\text{m}^3 \text{C}$

where τ_s is the carrier transport time across separate confinement heterostructure regions, τ_n is the bimolecular recombination lifetime, Γ is the optical confinement factor per well, β is the spontaneous emission factor, and ϵ is the gain compression factor. In addition, the optical gain function is expressed by a square dependence on the recombination current J_{nom} [10], $G = D(J_{\text{nom}} - 2 \times 10^{13})^2$, where D is a constant, $J_{\text{nom}} = I_n/V_a$, and V_a is the active layers volume. Table 1 lists all the parameters of the QW laser diode used in the simulation. Without feedback and modulation ($b = c = 0$), L – I curve simulation suggests a threshold current I_{th} of 38 mA. This agrees with a simple steady state analysis, in which the threshold current can be approximated as $(1 + \tau_s/\tau_n)(V_a N_0 + V_a/\sqrt{\Gamma R_p D})$. The step-response simulation (switching from 0 to a , where $a = 1.5I_{\text{th}}$) results in a relaxation oscillation f_r of 2.12 GHz and a period T of 0.471 ns.

To solve the delay differential equations, Eq. (2) can be expressed as $\dot{\mathcal{X}} = \mathcal{F}(t, \mathcal{X}) + A\mathcal{X}(t - \tau)$, where $\mathcal{X} \in R^3$ is the state variable $\mathcal{X} = (X^1, X^2, X^3) = (I_s, I_n, S_n)$, $\mathcal{F} = R \times R^3 \rightarrow R^3$ is a nonlinear function, and $A \in M^{3 \times 3}$ is a matrix with a nonzero term at a_{13} from Eq. (2). By modifying the fourth-order Runge–Kutta–Fehlberg method (RK45) [11] for fixed time step $\Delta (= \tau/n)$, we have

$$\begin{aligned} \mathcal{X}_m &= \varphi(\mathcal{X}_{m-1}, \mathcal{X}_{m-n}) \\ &= \mathcal{X}_{m-1} + \sum_{i=0}^5 c_i F_i^m, \end{aligned} \quad (3)$$

where

$$\begin{aligned}
 F_0^m &= \mathcal{F}(m\Lambda, \mathcal{X}_{m-1}) + A\mathcal{X}_{m-n}, \\
 F_i^m &= \mathcal{F}\left(m\Lambda + q_i, \mathcal{X}_{m-1} + \sum_{j=0}^{i-1} h_{ij}F_j^m\right) \\
 &\quad + A\left[\frac{A - q_i}{A}\mathcal{X}_{m-n} + \frac{q_i}{A}\mathcal{X}_{m-n+1}\right],
 \end{aligned}
 \tag{4}$$

and m is the time-step index ($m \geq n$), and c_i, q_i and h_{ij} are the coefficients of the RKF45 [11].

Fig. 2 shows the bifurcation diagram with S_n versus b when $a = 1.5I_{th}$, $\tau = 0.75T$, $c = 0.035$, and $f_0 = 1/2f_r$. In the three-dimensional phase diagram (I_s, I_n , and S_n) of the rate equations, let Σ be a two-dimensional hyperplane through a point (0.05, 0.0377, 0.4) with normal direction [0, 1, 0]. If the trajectory in the phase diagram mapped on the hyperplane densely fills out closed curve, then the solution forms a quasi-two-periodic orbit. When $b \in (0, 3.5)$ the system has a quasi-two-period attractor. When b varies from 0.41 to 0.45, the effects of quasi-periodicity route to chaos are observed.

Fig. 3a and b shows Poincaré maps at $b = 0.2$ and 0.44. When $b = 0$, the system has an asymptotically stable fixed point. As b increases to 0.2, the fixed point expands into an invariant closed-loop circle, a set like a circle which captures the point of a solution sequence. When $b = 0.44$, the circle breaks up into a complicated attracting set. These behaviors characterize the quasi-period and chaos in the system.

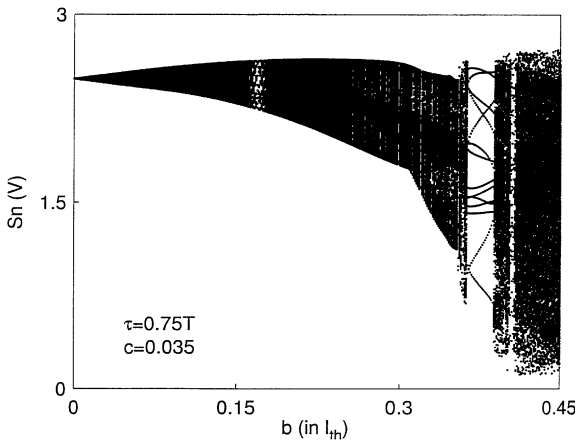


Fig. 2. Bifurcation diagram with S_n versus b when $a = 1.5I_{th}$, $\tau = 0.75T$, $c = 0.035$, and $f_0 = 1/2f_r$.

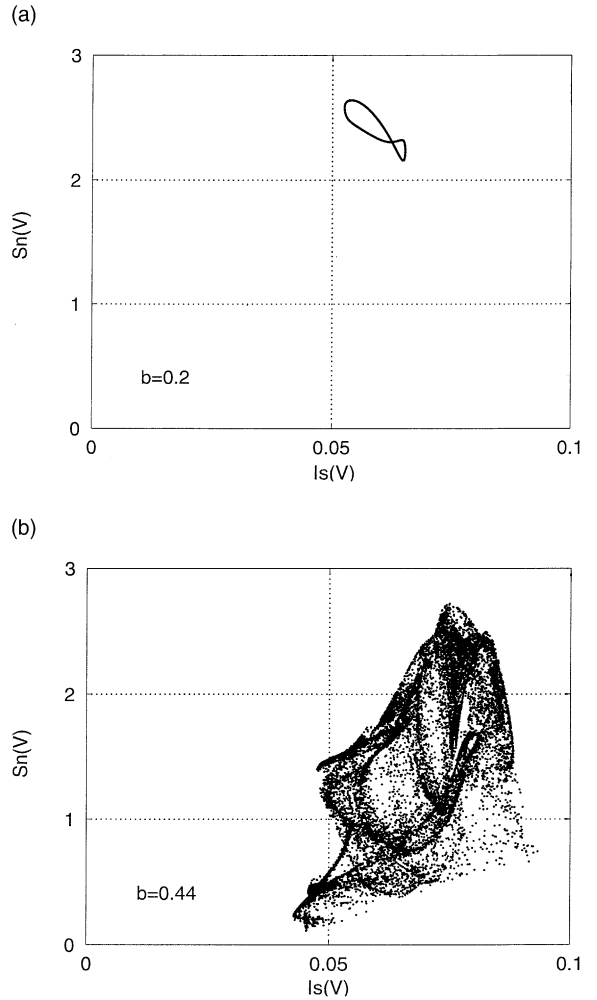


Fig. 3. (a,b) Poincaré maps at $b = 0.2$ and $b = 0.44$ when $a = 1.5I_{th}$, $\tau = 0.75T$, $c = 0.035$, and $f_0 = 1/2f_r$.

Lyapunov exponents are the generalization of the eigenvalues at an equilibrium point of characteristic multipliers. They can be used to determine the stability of quasi-periodic and chaotic behaviors, as well as that of equilibrium points and periodic solutions. Following the Farmer’s approach [12], a detailed formation to calculate the Lyapunov exponents for the delay differential equation are described by

$$\beta_l = \lim_{m \rightarrow \infty} \frac{1}{m} \ln |p_l(t)|,
 \tag{5}$$

where $p_l(t)$ is the l th eigenvalue of the Jacobian of $G^m(\mathcal{Y}_0)$. And,

$$\begin{aligned} \mathcal{Y}_m &= \begin{pmatrix} \mathcal{X}_m \\ \vdots \\ \mathcal{X}_{m+n-1} \end{pmatrix} = \begin{pmatrix} 0 & I & \cdots & \cdots & 0 \\ \vdots & 0 & I & & \vdots \\ \vdots & & \ddots & \ddots & \vdots \\ \vdots & & & \ddots & I \\ 0 & \cdots & \cdots & \cdots & 0 \end{pmatrix} \\ &\times \begin{pmatrix} \mathcal{X}_{m-1} \\ \vdots \\ \mathcal{X}_{m+n-2} \end{pmatrix} + \begin{pmatrix} 0 \\ \vdots \\ \varphi(\mathcal{X}_{m+n-2}, \mathcal{X}_{m-1}) \end{pmatrix} \\ &\equiv G(\mathcal{Y}_{m-1}), \end{aligned} \quad (6)$$

where $\mathcal{X}_m = \varphi(\mathcal{X}_{m-1}, \mathcal{X}_{m-n})$. Thus, the Jacobian of $G(\mathcal{Y}_{m-1})$ is given by

$$DG(\mathcal{Y}_{m-1}) = \begin{pmatrix} 0 & I & \cdots & \cdots & 0 \\ \vdots & \ddots & I & & \vdots \\ \vdots & & \ddots & \ddots & \vdots \\ 0 & \cdots & \cdots & 0 & I \\ D_y \varphi & 0 & \cdots & 0 & D_x \varphi \end{pmatrix}, \quad (7)$$

where

$$\begin{aligned} D_x \varphi(\mathcal{X}_{m+n-2}, \mathcal{X}_{m-1}) &= I + \sum_{i=0}^5 c_i D_x F_i^{m+n-1}, \\ D_x F_i^{m+n-1} &= (D\mathcal{F}) \left(I + \sum_{j=0}^{i-1} h_{ij} D_x F_j^{m+n-1} \right), \end{aligned} \quad (8)$$

and,

$$\begin{aligned} D_y \varphi(\mathcal{X}_{m+n-2}, \mathcal{X}_{m-1}) &= \sum_{i=0}^5 c_i D_y F_i^{m+n-1}, \\ D_y F_i^{m+n-1} &= (D\mathcal{F}) \left(\sum_{j=0}^{i-1} h_{ij} D_y F_j^{m+n-1} \right) + \delta_i A^{m+n-1}, \\ \delta_i A^{m+n-1} &\approx \\ &a_{13} \begin{pmatrix} 0 & 0 & (A - q_i)/A + (q_i X_m^{(3)}/A X_{m-1}^{(3)}) \\ 0 & 0 & 0 \\ 0 & 0 & 0 \end{pmatrix}. \end{aligned} \quad (9)$$

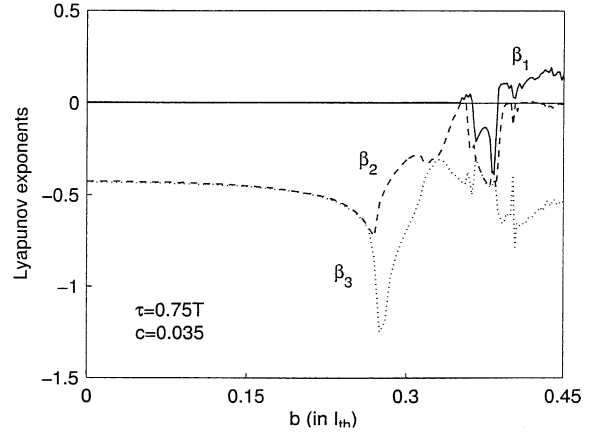


Fig. 4. The three Lyapunov exponents β versus b when $a = 1.5I_{th}$, $\tau = 0.75T$, $c = 0.035$, and $f_0 = 1/2f_r$.

Eqs. (3) and (5) are to be readily expanded to adaptive time step for improving the accuracy if necessary. If the delayed term $A = 0$, $D_y \varphi$ equals to zero. The eigenvalues of the Jacobian of $G^m(\mathcal{Y}_0)$ becomes the eigenvalues of $D_x \varphi$, which agrees with the conventional definition of the Lyapunov exponents.

Fig. 4 shows the three Lyapunov exponents β versus b when $a = 1.5I_{th}$, $\tau = 0.75T$, $c = 0.035$, and $f_0 = 1/2f_r$. Note that the second and the third Lyapunov exponent are all negative. $\beta_1 \approx 0$ when $b \in (0, 0.35)$. This implies a nonchaotic quasi two-period attractor which agrees with the results from Poincaré maps. Because at least one Lyapunov exponent of a chaotic system must be positive, chaotic behavior can be established in regions where one positive Lyapunov exponent is shown in the figure. The system also has a chaotic window for $b \in (0.364, 0.386)$, therefore, in this region there is no positive Lyapunov exponent.

In conclusion, it is proposed that a delayed-feedback technique is used to achieve route to chaos in a quantum-well laser diodes at relatively low bias and small modulation depth. Quasi-periodicity route to chaos can be visualized by the bifurcation diagram and Poincaré map, and further be supported by the calculation of Lyapunov exponents for the delay differential rate equation.

References

- [1] C.R. Mirasso, P. Colet, P. Garcia-Fernandez, Synchronization of chaotic semiconductor lasers: application to encoded communications, *IEEE Photon. Technol. Lett.* 8 (1996) 299.
- [2] V. Annovazzi-Lodi, S. Donati, A. Scire, Chaos and locking in a semiconductor laser due to external injection, *IEEE J. Quant. Electron.* 33 (1997) 1449.
- [3] I. Fischer, O. Hess, W. Elsässer, Göbel, High-dimensional chaotic dynamics of an external cavity semiconductor laser, *Phys. Rev. Lett.* 73 (1994) 2188.
- [4] V. Kovanis, A. Gavrielides, T.B. Simpson, J.M. Liu, Instabilities and chaos in optically injected semiconductor lasers, *Appl. Phys. Lett.* 67 (1995) 2780.
- [5] S. Bennett, C.M. Snowden, S. Iezekiel, Nonlinear dynamics in directly modulated multiple-quantum-well laser diodes, *IEEE J. Quant. Electron.* 33 (1997) 2076.
- [6] E. Hemery, L. Chusseau, J.M. Lourtioz, Dynamic behaviors of semiconductor lasers under strong sinusoidal current modulation: modeling and experiments at 1.3 μm , *IEEE J. Quant. Electron.* 26 (1990) 633.
- [7] P. Saboureau, J.-P. Foing, P. Schanne, Injection-locked semiconductor lasers with delayed optoelectronic feedback, *IEEE J. Quant. Electron.* 33 (1997) 1582.
- [8] D. Pieroux, T. Erneux, A. Gavrielides, V. Kovanis, Hopf bifurcation subject to large delay in a laser system, *SIAM J. Appl. Math.* 61 (2000) 966.
- [9] M.F. Lu, J.S. Deng, C. Juang, M.J. Jou, B.J. Lee, Equivalent circuit model of quantum well lasers, *IEEE J. Quant. Electron.* 31 (1995) 1418.
- [10] R.S. Tucker, Large-signal circuit model for simulation of injection laser modulation dynamics, *IEEE Proc.* 128 (1981) 180.
- [11] D. Kincaid, W. Cheney, *Numerical Analysis*, Brooks/Cole, Pacific Grove, 1991.
- [12] J.D. Farmer, Chaotic attractors of an infinite-dimensional dynamical system, *Physica D* 4 (1982) 366.